Smart Structures and Systems, *Vol. 26, No. 1 (2020) 63-75*
DOI: https://doi.org/10.12989/sss.2020.26.1.063

ANN based on forgetting factor for online model updating in substructure pseudo-dynamic hybrid simulation

Yan Hua Wang*, Jing Lv [a], Jing Wu [b] and Cheng Wang [c]

Key Laboratory of Concrete and Prestressed Concrete Structures of Ministry of Education, Southeast University, China

(*Received October 11, 2019, Revised January 19, 2020, Accepted May 4, 2020*)

Abstract. Substructure pseudo-dynamic hybrid simulation (SPDHS) combining the advantages of physical experiments and numerical simulation has become an important testing method for evaluating the dynamic responses of structures. Various parameter identification methods have been proposed for online model updating. However, if there is large model gap between the assumed numerical models and the real models, the parameter identification methods will cause large prediction errors. This study presents an ANN (artificial neural network) method based on forgetting factor. During the SPDHS of model updating, a dynamic sample window is formed in each loading step with forgetting factor to keep balance between the new samples and historical ones. The effectiveness and anti-noise ability of this method are evaluated by numerical analysis of a six-story frame structure with BRBs (Buckling Restrained Brace). One BRB is simulated in OpenFresco as the experimental substructure, while the rest is modeled in MATLAB. The results show that ANN is able to present more hysteresis behaviors that do not exist in the initial assumed numerical models. It is demonstrated that the proposed method has good adaptability and prediction accuracy of restoring force even under different loading histories.

Keywords: substructure pseudo-dynamic hybrid simulation; online model updating; artificial neural network; forgetting factor

1. Introduction

Substructure pseudo-dynamic hybrid simulation (SPDHS) (Nakashima and Takai 1985, Dermitzakis and Mahin 1985) combining the advantages of physical testing methods and numerical simulation, is widely used in the field of seismic engineering (Kim *et al*. 2011, Spencer *et al*. 2014). In recent decades, SPDHS has focused on several key issues, including time integration algorithm (Wu *et al*. 2005, 2006, Chen *et al*. 2009, Zakersalehi *et al*. 2019), rate-dependent real-time hybrid simulation (Nakashima *et al*. 1992, Tang *et al*. 2016), actuator control (Phillips and Spencer 2013, Wu and Zhou 2014), time-delay compensation (Darby *et al*. 2002, Wang *et al*. 2019, Carrion *et al*. 2009), remote network collaborative hybrid simulation (Kwon *et al*. 2008), boundary condition (Wu *et al*. 2018, Ning *et al*. 2019), etc.

Generally, some key components or sections which enter into nonlinear failure easily are taken as experimental substructures to conduct physical tests, while the rest components are modeled in numerical simulation, as illustrated in Fig. 1. Due to equipment restrictions, only one or a few representative components can be selected to execute physical tests. However, when the proportion of nonlinear components in the numerical substructure increases, the model errors may accumulate to a non-negligible level that seriously affects the global performance of the entire structure. Therefore, how to effectively improve the model accuracy in SPDHS is an urgent problem to be solved.

The concept of model updating was first introduced into substructure pseudo-dynamic hybrid simulation by Kwon and Kammula (2013), in which the numerical models were modeled with Bouc-Wen-Baber-Noori (BWBN) models and shared similar hysteresis behaviors with experimental substructure. The numerical models were online updated by the data from the experimental substructure. A weighting coefficient was determined for each numerical model until the sum of their weighted responses coincided with the measured experimental responses. In recent decades, various model updating techniques have been introduced into SPDHS to improve the accuracy of numerical models based on the reliable data from experimental substructure. The model updating methods in SPDHS can be roughly divided into two categories: parameter identification methods and artificial neural network (ANN) methods. The parameter identification methods mainly contain the nonlinear multivariate optimization algorithms (the gradient method by Chuang *et al*. (2018), NedMead-Simplex method by Yang *et al*. (2012), etc.), least squares algorithm (Zhang *et al*. 2011), unscented Kalman filter (UKF) method (Hashemi *et al*. 2014, Shao *et al*. 2016), and constrained unscented Kalman filter (CUKF) method (Wang and Wu 2013, Wu and Wang 2014, Ou *et al*. 2017). For a parameter

*Corresponding author, Associate Professor,
E-mail: 101010371@seu.edu.cn
[a] Master Student, E-mail: 220171064@seu.edu.cn
[b] Professor, E-mail: seuwj@seu.edu.cn
[c] Master Student, E-mail: wangchengkyrie@outlook.com

ISSN: 1738-1584 (Print), 1738-1991 (Online)

identification method, when there are not enough parameters to identify the specific nonlinear behaviors of the structure or component, the model gap between the assumed models and the actual models cannot be avoided fundamentally. In contrast, ANN (artificial neural network) can be applied to directly fit the constitutive models and acquire more hysteresis information that does not exist in the initial assumed numerical models. Thus, the ANN methods are necessary supplements to the parameter identification methods.

In the past decades, the ANN methods have been gradually explored. Yang and Nakano (2005) applied neural network as a regression tool to update the numerical models in the numerical substructure. Yun *et al.* (2008a, b) proposed a five-eigenvector input for ANN to fit hysteresis model, and identified the constitutive model of steel frame column joints based on ANN method. The numerical simulation results showed that stiffness degradation and contraction of the hysteresis loop can be well recognized by ANN. Elanwar and Elnashai (2016) adopted offline neural network algorithm to identify the bilinear constitutive model of a two-span steel frame, which was executed offline without step-by-step model updating. Moreover, Wang *et al*. (2017) applied online neural network algorithm to model updating in SPDHS. Only the experimental substructure data in the current loading step was collected for online model updating. The numerical simulation verified the feasibility of online neural network algorithm for model updating in SPDHS.

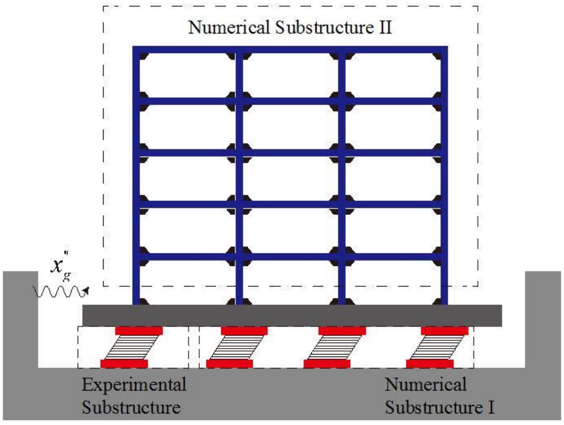

Fig. 1 A frame structure with isolations

However, the online neural network algorithm has poor resistance to occasional bad samples and cannot ensure good stability. Therefore, in this study, a dynamic sample window with a certain length is used to online train ANN model for well stability, in which the experimental substructure data is collected for training. To guarantee adaptability, a forgetting factor is introduced to keep balance between the latest samples and historical ones, so as to prevent the latest samples being obliterated by the historical samples. In this proposed method, the structural component that is expected to exhibit nonlinear hysteresis first is selected as the experimental substructure.

In this study, ANN is first pre-trained offline by the experimental substructure data collected from traditional SPDHS, in which some hysteresis behaviors can be learned in advance to ensure the prediction accuracy of restoring force. And the pre-trained ANN model is set as the initial model of component with similar hysteresis relationship in numerical substructure for online model updating subsequently. Then, during online model updating in SPDHS, a dynamic sample window with forgetting factor is generated in each loading step to online train the ANN model. The ANN model will be gradually fine tuned to a more accurate one according to the physical substructure data.

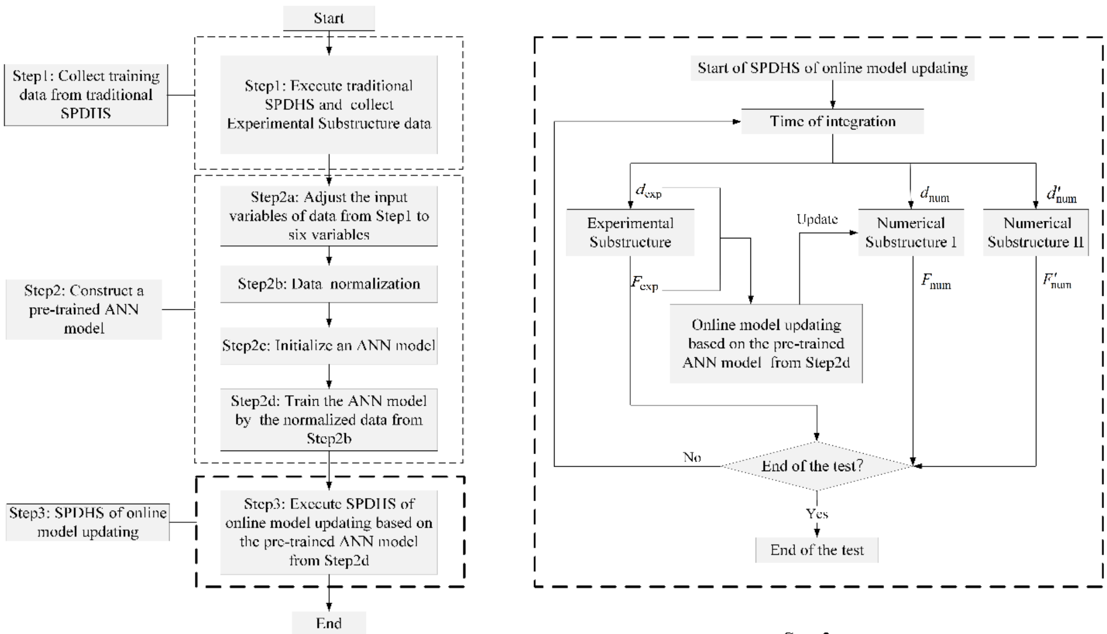

Step3

The main steps of the proposed methodology

Fig. 2 Framework of the proposed methodology

2. Implementation of the proposed methodology

Time integration scheme, data exchange between the numerical models and the experimental specimen are included in traditional SPDHS. In the proposed model updating method, the offline pre-trained step and online model updating procedure are added to the traditional SPDHS. A frame structure with isolations in Fig. 1 is taken as an example to illustrate the framework and implementation of the proposed methodology, which mainly contains three steps shown in Fig. 2. It is assumed that the components in Numerical Substructure I share similar hysteresis relationship with Experimental Substructure.

The specific procedures are summarized as follows:

Step1 Execute traditional SPDHS and collect Experimental Substructure data:

The traditional SPDHS is executed as preliminary hybrid simulation. The numerical models of elements in Numerical Substructure I are assumed numerical models with model errors. The Experimental Substructure data including displacements and restoring forces are collected for Step2.

Step2 Construct a pre-trained ANN model:

To get knowledge of the loading history and hysteresis information of Experimental Substructure in advance, an ANN model is pre-trained offline by the collected Experimental Substructure data from Step1. Generally, when there is large model gap between the assumed numerical models and the real models in the Numerical Substructure I, it is necessary to carry out traditional SPDHS in Step1. Therefore, some hysteresis information about the Experimental Substructure can be acquired in advance to ensure the accuracy of model updating. The detailed procedure of Step2 are listed as follows:

(a) Adjust the input variables of Experimental Substructure data from Step1 to six variables:

The Experimental Substructure data including displacements and restoring forces from Step1 are processed to make the hysteresis relationship a one-to-one nonlinear mapping by adjusting the input variables. For the nonlinear time-delay dynamic system in this study, the displacement input and the restoring force output correspond to a nonlinear time series. The restoring force in the current loading step is not only related to the displacement in the current loading step, but also to the historical restoring forces and displacements. Thus, the input variables for the hysteresis model are adopted as shown in Eq. (1)

$$F_i = \varphi(d_i, d_{i-1}, F_{i-1}, d_{i-1} \bullet F_{i-1}, F_{i-1} \bullet \Delta d_i, E_{i-1}) \quad (1)$$

where F_i and d_i represent the restoring force and displacement in the i-th loading step respectively; $\Delta d_i = d_i - d_{i-1}$; $E_{i-1} = E_{i-2} + |F_{i-1} \bullet d_{i-1}|$, E_{i-1} (Kim *et al.* 2012) represents the cumulative energy dissipation up to the (i-1)-th loading step.

The input variables of the Experimental Substructure data from Step1 are adjusted to six variables shown in Eq. (1), which are used for subsequent offline neural network training.

(b) Data normalization:

Since the data distribution of each variable in Eq. (1) may be quite different, it is possible to appear non-convergence when training ANN model. Therefore, it is necessary to normalize the input variables and output variable to map them to the interval [0, 1]. For example, variable X is normalized to X'

$$X' = \frac{X - min(X)}{max(X) - min(X)} \quad (2)$$

(c) Initialize an ANN model:

An ANN model is established with random initialization of weights and thresholds. The structural parameters of ANN model mainly include the number of hidden layers, the number of neurons in each hidden layer and the variables in the input layer. In general, the learning ability of ANN model is dependent on the structural parameters.

(d) Train the ANN model by the normalized data:

The initialized ANN model from Step2(c) is offline trained by the normalized Experimental Substructure data from Step2(b). And the pre-trained ANN model is set as the initial hysteresis model of component in Numerical Substructure I for the subsequent SPDHS of online model updating.

Step3 SPDHS of online model updating:

In this step, SPDHS of online model updating is executed as shown in Fig. 2. The initial model of component in Numerical Substructure I is set to the pre-trained ANN model in Step2d. Because there are still some prediction errors of restoring force between the pre-trained ANN model and the real model, the pre-trained ANN model of component in Numerical Substructure I is still needed to be online fine tuned to a accurate one during SPDHS of online model updating. The specific procedures are summarized as follows:

(a) Numerical integration of equation of motion:

According to the global responses in the previous loading step, based on the equation of motion of the entire structure, the displacement of each substructure in the next loading step is solved by numerical integration scheme. The displacements of Experimental Substructure, Numerical Substructure I, and Numerical Substructure II in the next loading step are set to d_{exp},d_{num}, and d'_{num} respectively. After inputting the displacements of Experimental Substructure and Numerical Substructure II, the restoring force of Experimental Substructure can be measured as F_{exp}, and the restoring force of Numerical Substructure II can also be calculated as F'_{num} directly. It is worth noting that the measured Experimental Substructure data will be applied to online calibrate the inaccurate ANN model of component in Numerical Substructure I.

(b) Experimental Substructure data normalization:

The input variables of Experimental Substructure data in the current loading step are adjusted to six variables as shown in Eq. (1). The input variables and output variable are normalized to the interval [0, 1]. The processing method refers to Eq. (2), in which the maximum and minimum values are the ones obtained from Step2 (b).

(c) Numerical Substructure I data normalization:

Similarly, the input variables of Numerical Substructure I data in the current loading step are also supposed to be adjusted to six variables as shown in Eq. (1). Then, the input variables are normalized to the interval [0, 1] as shown in Eq. (2) for unified data processing.

(d) The selection of online training data

The latest Experimental Substructure data is applied to form a dynamic sample window with forgetting factor in each loading step for online training the ANN model. The detailed selection of online training data will be discussed as follows:

Standard artificial neural network is usually trained by all the samples which are collected from the beginning to the current loading step. The required resource of the PC system increases with the trained samples. When the samples reach a certain number, it will put much pressure on the system and result in inefficiency. On the other hand, if merely one sample is applied to train ANN model in each loading step, it may easily converge at the local minimum point even with fast training speed. Moreover, the ability of ANN to resist the interference of bad samples is unsatisfactory, which may result in poor robustness and stability. Therefore, the proper samples for online training ANN model are the latest small batch samples of Experimental Substructure which are gathered up to the current loading step.

It should be noted that the newly added samples with more new hysteresis information have not been trained, while the historical samples have been trained many times. Therefore, there is a risk that the newly added samples will be obliterated by the historical samples, which will reduce the adaptability of online model updating. In order to improve the adaptability of online model updating, a forgetting factor is introduced to increase the training weight of the newly added samples. A dynamic sliding window of samples with forgetting factor is selected for stepwise online training of ANN model.

The latest small batch samples are placed in the dynamic sample window with a fixed length of L. When the newest sample is input, the earliest historical sample is removed simultaneously. The samples of Experimental Substructure enter and exit the dynamic sliding window according to a first-in-first-out protocol. A dynamic sliding window with a fixed number L can be expressed as follows

$$window = [(X_1, Y_1), \cdots, (X_L, Y_L)] \tag{3}$$

where (X_1, Y_1) is the earliest historical sample, while(X_L, Y_L) is the newest input sample. At the same time, the loss function of the ANN model is set as

$$E' = \sum_{m=1}^{L} \omega_m {e_m}^2 \tag{4}$$

where e_m and ω_m are the training error and the weight coefficient of the m-th sample respectively. The weight coefficient ω_m is determined by the exponential forgetting method

$$\omega_m = \frac{1-\mu}{1-\mu^L}\mu^{L-m} \tag{5}$$

where μ denotes the forgetting factor, and $\sum_{m=1}^{L} \omega_m = 1$.

(e) Online train the ANN model:

The weighted samples in the dynamic sample window are input into the ANN model trained in the previous loading step for continuous training.

(f) Restoring force prediction:

The normalized six input variables of Numerical Substructure I from Step3(c) are input into the trained ANN model in Step3(e) to predict the dimensionless restoring forces of elements in Numerical Substructure I. The dimensionless restoring forces are needed to be reversely normalized to acquire desired the restoring forces F_{num}. Then the restoring forces of the three substructures (Experimental Substructure, Numerical Substructure I, Numerical Substructure II) are fed back to the equation of motion. The above procedures in Step3 are repeated until the ground motion input is completed.

3. Numerical validation

Firstly, the hysteresis model and ANN configurations for numerical validation are introduced. Then, the SPDHS of online model updating of a six-story frame structure with BRBs (Buckling Restrained Brace) is conducted, in which the effectiveness and anti-noise ability of the proposed method is demonstrated. Moreover, the results of preliminary hybrid simulation and offline calibration are discussed. Finally, the performance of the proposed method in another ground motion is executed to verify the generality of the proposed method.

3.1 Hysteresis model for numerical validation

In this study, Bouc-Wen-Baber-Noori (BWBN) model with strength degradation, stiffness degradation, and pinching (Baber and Noori 1985) is taken as the real model of Experimental Substructure. It is assumed that the components in Numerical Substructure I share similar constitutive properties with Experimental Substructure.

The restoring force F consists of two parts: the linear part related to the structural displacement d and the hysteresis part related to plastic displacement z. The expression of F is as follows

$$F = \alpha k_0 d + (1-\alpha) k_0 z \tag{6}$$

where F denotes the restoring force, d is the structural displacement, α is the ratio of the post-yielding stiffness to elastic stiffness, k_0 is the elastic stiffness, $z$represents the plastic displacement. The plastic displacement z is used to describe the degradation and pinching behaviors. The rate of z can be written in the following form

$$\dot{z} = h(z)\left\{\frac{A(\varepsilon)\dot{d} - \nu(\varepsilon)\left[\beta\left|\dot{d}\right||z|^{n-1}z + \gamma\dot{d}|z|^n\right]}{\eta(\varepsilon)}\right\} \tag{7}$$

Table 1 The role of parameters in BWBN model

Parameters	Physical meaning
k_0	Initial elastic stiffness
α	The ratio of the post-yielding to elastic stiffness
A β γ n δ_A	Hysteresis loop shape
δ_v	Strength degradation parameter
δ_η	Stiffness degradation parameter
ζ_s p q Ψ δ_Ψ λ	Pinching parameters

$$A(\varepsilon) = A_0 - \delta_A \varepsilon \tag{8}$$

$$\nu(\varepsilon) = 1 + \delta_\nu \varepsilon \tag{9}$$

$$\eta(\varepsilon) = 1 + \delta_\eta \varepsilon \tag{10}$$

$$\dot{\varepsilon} = (1 - \alpha) k_0 \dot{d} z \tag{11}$$

where A, β, γ and n control the shape of the hysteresis loop, $\nu(\varepsilon)$ and $\eta(\varepsilon)$ are the degradation parameters given by Eqs. (9)-(10). δ_A, δ_ν and δ_η are the degradation parameters, and the rate of ε is defined in Eq. (11). $h(z)$ represents the material pinching parameter described in Eq. (12).

$$h(z) = 1 - \zeta_1 \, exp\left[-\left(\frac{z \operatorname{sgn}(\dot{d}) - q z_{max}}{\zeta_2}\right)^2\right] \tag{12}$$

$$\zeta_1 = \zeta_s [1 - exp(-p\varepsilon)] \tag{13}$$

$$\zeta_2 = (\Psi + \delta_\Psi \varepsilon)(\lambda + \zeta_1) \tag{14}$$

$$z_{\max} = \left[\frac{A}{\nu(\beta + \gamma)}\right]^{\frac{1}{n}} \tag{15}$$

where ζ_s, p, q, Ψ, δ_Ψ, and λ are the pinching parameters. The role of these parameters in BWBN model is summarized in Table 1.

3.2 Model description and ANN configurations

The structural model adopted in this numerical study will be described in section 3.2.1. And the ANN configurations in the proposed methodology are discussed in section 3.2.2.

3.2.1 Model description

The SPDHS of a six-story frame structure with BRBs is fully simulated as shown in Fig. 3. The 270 × 270 × 9 × 14 hot-rolled H-beam (Q345) is used for all the frame columns and beams. The columns at the first story are fixed to the base. The following assumptions are adopted: the stiffness of all the beams is infinite; the entire structure is calculated by the interlaminar shear model; the total 12 BRBs with similar hysteresis relationship are hinged to the entire frame structure, and only the axial deformation is considered.

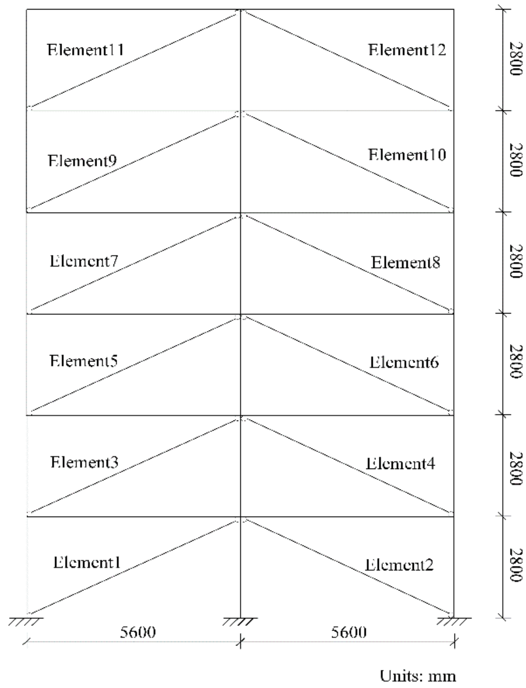

Fig. 3 A frame structure with BRBs

In the fully simulated SPDHS, the entire structure is divided into three substructures: the left BRB (Element 1) at the first story is regarded as the Experimental Substructure, the other 11 BRBs (Elements 2-12) are placed in Numerical Substructure I and the frame structure is left in Numerical Substructure II. The Experimental Substructure is modeled with two-node-link element in OpenFresco (Schellenberg *et al*. 2009) without specimen executed physically. The other 11 BRBs and the frame structure are simulated in the computational driver MATLAB@ (2018). The information between OpenFresco and MATLAB is exchanged online through TCP sockets. The boundary conditions of the three parts are unified in the equation of motion. The BWBN models considering degradation and pinching behaviors are utilized as the real models of the total 12 BRBs and the specific parameters are shown in Table 2.

Moreover, it is assumed that the lumped mass of the intermediate node at each story is 100 t, while the lumped mass of the other nodes at each story is set to 50 t. The uniformly distributed load on the beam at each story is set to 30 kN/m. The nonlinear $P - \Delta$ effects are considered in this study. The Rayleigh damping is adopted and the damping coefficient is set to 0.05 at first and second modes. Explicit Newmark time integration scheme is applied to solve the equation of motion, and the integral step is set to 0.01 s. The basic natural period of the structure is 0.398 s. The north-south component of ground motion recorded in El Centro during the Imperial Valley earthquake on May 18, 1940 is selected as the external seismic excitation, in which the PGA is adjusted to 1000 gal and the sample time interval is set to 0.01 s. Then the global dynamic responses of the structure are step by step solved with Explicit Newmark time integration scheme under the earthquake load.

Table 2 Parameters of the BWBN model of the total 12 BRBs

k_0 (N/mm)	α	A	β	γ	n	δ_A	δ_ν	δ_η	ζ_s	p	q	Ψ	δ_Ψ	λ
74227	0.01	1	1.8	0.8	1	0	5×10^{-9}	5×10^{-9}	0.95	4	0.25	0.6	0.5	1

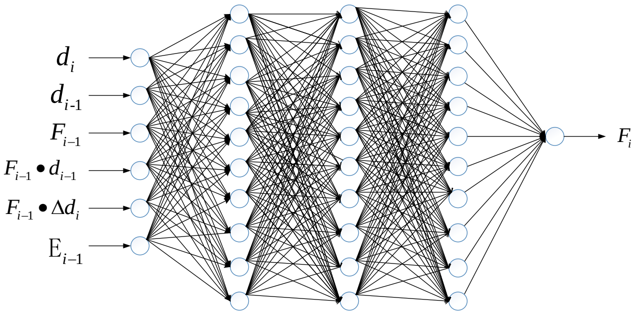

Fig. 4 Structure of ANN model with three hidden layers

3.2.2 ANN configurations

The ANN configurations in this numerical validation will be discussed in detail. The ANN model is established and trained by the Neural Network Toolbox (2018) in MATLAB@.

In Setp2c, to ensure that ANN can learn enough complex nonlinear behaviors, it is assumed that the number of hidden layer is 3 and the number of neurons in all the hidden layers is 10. The input variables in Eq. (1) are adopted in the input layer. The structure of ANN model adopted in this numerical study is shown in Fig. 4.

The loss function of ANN training algorithm is set to mean square error (MSE). In order to reduce the loss function effectively, the Levenberg-Marquardt (LM) algorithm (Moré 1978) is selected to adjust the connection weights and thresholds. The LM algorithm combines the advantages of Gauss-Newton method and gradient descent method. The rule of connection weight modification of LM algorithm is

$$W_{k+1} = W_k - (J^T J + \nu I^{-1}) J^T e \tag{16}$$

where W_{k+1} denotes the connection weight vector in the $k+1$ iteration. ν represents the control factor that determines the step size of gradient descent. When ν is small, LM algorithm is close to the Gauss Newton method. On the contrary, when ν increases to a large value, LM algorithm approaches the gradient descent method. J is the Jacobian matrix of the derivation of the weight by the error vector e, I is the unit matrix.

In Setp2d, the Experimental Substructure data from preliminary hybrid simulation is divided into two parts: 75% for training and 25% for testing. Then, an ANN model with random initial weights and thresholds is offline trained. The control factor$\boldsymbol{\nu}$and the maximum iteration of LM algorithm is set to 0.001 and 1000 respectively.

In Setp3, the pre-trained ANN model is gradually fine tuned to a more accurate one in the SPDHS of online model updating. In order to prevent the gradient from falling too fast, the control factor ν of LM algorithm should be set to a small value. Moreover, in order to prevent the weights and thresholds of ANN model from being damaged by occasional bad samples, it is necessary to use less iterative steps to ensure the stability of the system. Thus, in the SPDHS of online model updating, the control factor ν of LM algorithm is set to a small value 10^{-5} and the maximum iteration is set to 2. In addition, the length L of the sliding dynamic sample window is fixed at 200 in each loading step, and the forgetting factor is set to 0.1.

3.3 Numerical simulation results

In this section, firstly, the effectiveness of the proposed method is demonstrated in section 3.3.1. Then, the preliminary hybrid simulation results and performance of offline calibration will be discussed in section 3.3.2 and section 3.3.3 respectively. Next, the anti-noise ability of the proposed method is evaluated in section 3.3.4. Finally, the performance of the proposed method in another ground motion is estimated in section 3.3.5.

3.3.1 The effectiveness of the proposed method

The effectiveness of the proposed method is validated with five types of SPDHS: (i) Reference SPDHS, (ii) Traditional SPDHS, (iii) online model updating SPDHS with the proposed method in this paper, (iv) online model

Table 3 Five simulation cases for numerical analysis

Case	Type of simulation	Model of Element 1	Initial models of Elements 2-12	Model updating method
Reference	Reference SPDHS	BWBN	BWBN	-
Traditional	Traditional SPDHS	BWBN	Bilinear	-
ANN1	Online model updating SPDHS with the proposed method	BWBN	Bilinear	ANN with forgetting factor
ANN2	Online model updating SPDHS with traditional ANN method	BWBN	Bilinear	Traditional ANN
UKF	Online model updating SPDHS with UKF method	BWBN	Bilinear	UKF

updating SPDHS with traditional ANN method, and (v) online model updating SPDHS with UKF method. The specific configurations of the five simulation cases are listed in Table 3. It is supposed that the constitutive model of Experimental Substructure (Element 1) is BWBN model as shown in Table 2 in five simulation cases. And the models of elements in Numerical Substructure I (Elements 2-12) share similar hysteresis relationship with Experimental Substructure.

Table 4 Parameters of the Bilinear model

k_0 (N/mm)	α	F_y (N)
68000	0.008	35000

In Reference case, the models of Elements 2-12 are set to BWBN models as shown in Table 2. In Traditional case, the models of Elements 2-12 are set to Bilinear ones as shown in Table 4. In ANN2 case, the length L of the sliding dynamic sample window is set to 1 (only the current loading step) without forgetting factor. As a comparison, in ANN1 case, the length L and forgetting factor are set to 200 and 0.1 respectively. In UKF case, a state vector to be identified is defined as

$$Z = [k_0, \alpha, F_y] \tag{17}$$

where the initial value of Z is shown in Table 4, F_y denotes the yield strength. In addition, it is assumed that the initial state covariance matrix P_0, the process noise

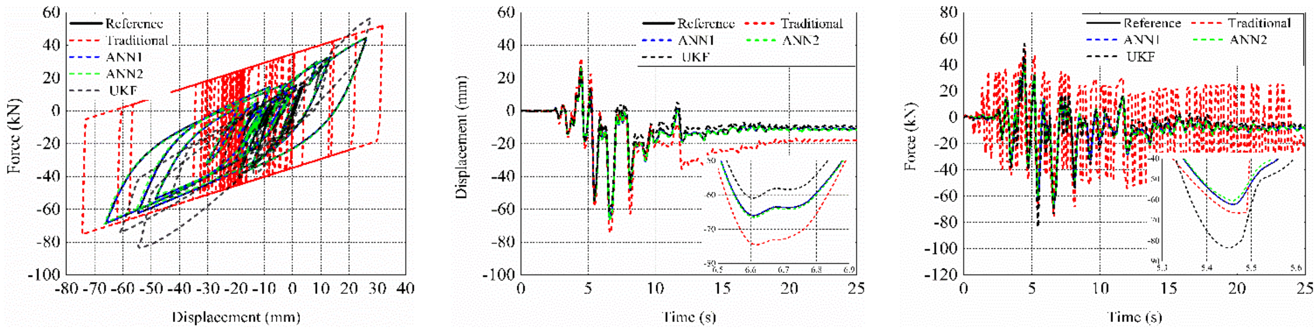

(a) Hysteresis curve (b) Displacement history (c) Restoring force history

Fig. 5 Comparison of predicted responses of Element 2 at the first story in different cases

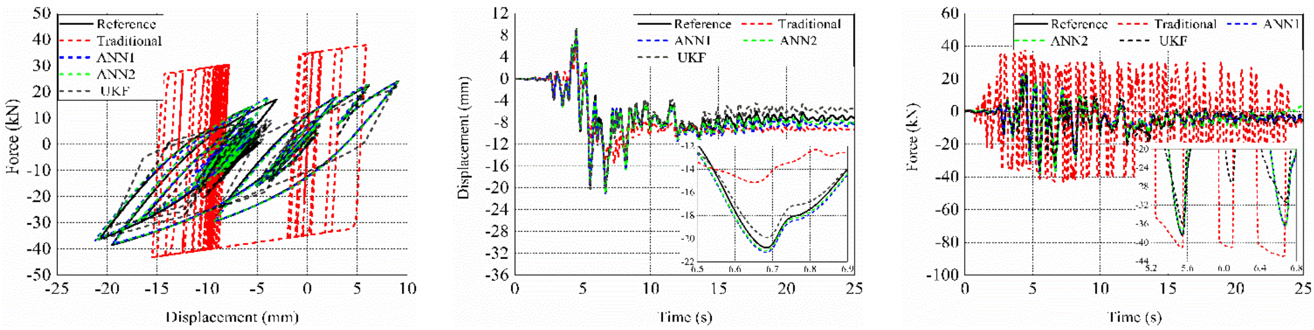

(a) Hysteresis curve (b) Displacement history (c) Restoring force history

Fig. 6 Comparison of predicted responses of Element 6 at the third story in different cases

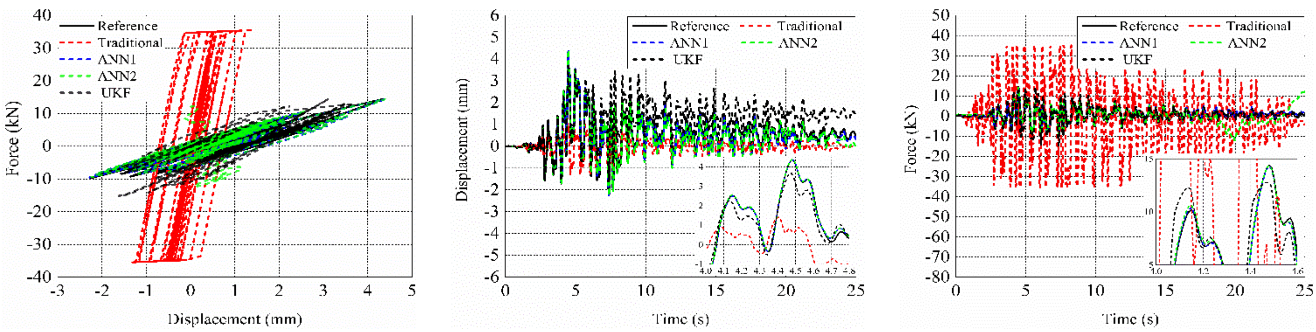

(a) Hysteresis curve (b) Displacement history (c) Restoring force history

Fig. 7 Comparison of predicted responses of Element 10 at the fifth story in different cases covariance matrix Q and the measurement noise covariance matrix R are set to

$$P_0 = diag([10^{-8}, 0.1, 0.1]) \tag{18}$$

$$Q = diag([0,0,0]) \tag{19}$$

$$R = [10^{-9}] \tag{20}$$

Since the structure is symmetrical, only the BRBs on right side of structure are analyzed and discussed, especially some typical members (Element 2, Element 6, Element 10). Comparison of the predicted hysteresis curves, displacement histories and restoring force histories of Element 2, Element 6, Element 10 in five simulation cases are illustrated in Figs. 5-7. Moreover, the peak responses in the time histories are shown in an enlarged view to better discuss the performance of different model updating cases.

Fig. 5 shows the comparison of the predicted hysteresis curves, displacement histories and restoring force histories of Element 2 in five simulation cases. It is noted that the loading history of Element 2 is consistent with the one of Element 1 (Experimental Substructure). It is obvious that the hysteresis models updated in ANN1 case and ANN2 case coincide with the reference models. ANN is shown to be able to learn degradation and pinching behaviors which do not exist in the initial Bilinear model. In contrast, there are large deviations of the models from the reference ones in UKF case. It may be due to the absence of corresponding parameters to identify the complex nonlinear behaviors of elements. Moreover, the displacement and restoring force histories in ANN1 case and ANN2 case are also in good agreement with those of the reference ones, especially at the peak. The displacement and restoring force histories predicted in UKF case deviate a little from the real ones. And the absolute errors of predicted displacement and restoring force at the peak are 6.914 mm and 22.147 kN respectively. It implies that there maybe large errors in the prediction of restoring force in UKF case, when the inherent model gap exists between the initial numerical models and the real ones.

Fig. 6 shows the comparison of the predicted hysteresis curves, displacement histories and restoring force histories of Element 6. Similarly, the predicted hysteresis models and dynamic responses in ANN1 case are consistent with the real ones. However, it is shown that the restoring force history in ANN2 case deviates from the true value at 22.3 s. It may be due to the difference of the loading histories between Element 6 and Element 1 (Experimental Substructure). This can result in the decrease of prediction accuracy and adaptability of the traditional ANN method. In UKF case, the prediction errors of displacement and restoring force at the peak are 4.562 mm and 16.590 kN respectively, which are larger than the ones in ANN1 case and ANN2 case.

As shown in Fig. 7, the hysteresis models and dynamic responses in ANN1 case still coincide with the reference ones. The proposed method has good prediction accuracy of restoring force and adaptability under different loading histories. In contrast, the restoring force history in ANN2 case diverges at 18.6 s. It suggests that the traditional ANN method is relatively sensitive to the difference of loading histories, thus the prediction accuracy of restoring force cannot be guaranteed. In UKF case, the absolute prediction errors of displacement and restoring force at the peak responses are still the largest in the three model updating cases. It can be concluded that the prediction errors in UKF case mainly come from the inherent model gap between the initial numerical models and the real ones.

In order to evaluate the prediction accuracy of restoring force quantitatively, the prediction errors of the restoring force in the three model updating cases are illustrated in Fig. 8. Furthermore, the maximum absolute errors and *RMSD* (The Root Mean Square Deviation) of restoring force prediction are listed in Table 5. *RMSD* represents the accumulation of deviation of restoring force prediction over time. The expression is as follows

$$RMSD_i = \sqrt{\frac{\sum_{j=1}^{i}(F_j^{exact} - \hat{F}_j)^2}{\sum_{j=1}^{i}(F_j^{exact})^2}} \tag{21}$$

where F_j^{exact} denotes the true value of restoring force in the j-th loading step, $\hat{F}_j$ is the predicted restoring force in the j-th loading step, and $(F_j^{exact} - \hat{F}_j)^2$ represents the cumulative value of square of restoring force prediction errors from the beginning to the current loading step.

Fig. 8 presents the prediction errors of restoring force of three elements in the three model updating cases. It can be seen that the force error curves of three elements in ANN1 case approach to zero lines. The proposed method in this paper works well in model updating. In ANN2 case, the force error curve of Element 2 fluctuates slightly near the

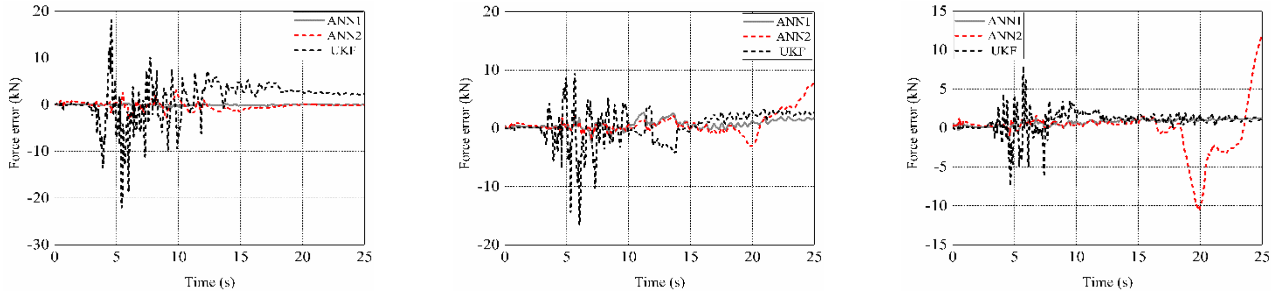

(a) Element 2 (b) Element 6 (c) Element 10

Fig. 8 Comparison of restoring force prediction errors of three elements

Table 5 Summary of restoring force prediction errors of Element2-Element12

Story	Element	Maximum absolute error			RMSD (at 25s)		
		ANN1 (kN)	ANN2 (kN)	UKF (kN)	ANN1	ANN2	UKF
1	Element 2	1.261	3.321	22.147	0.0142	0.0571	0.2847
2	Element 4	2.980	3.552	12.290	0.0725	0.1085	0.2756
3	Element 6	2.696	8.136	16.590	0.1158	0.2233	0.3321
4	Element 8	2.132	11.923	13.092	0.2236	0.5107	0.4042
5	Element 10	1.295	12.140	7.915	0.2780	1.0103	0.5517
6	Element 12	0.683	11.540	4.970	0.1926	2.0218	0.4466

zero line. However, as seen in Figs. 8(b)-(c), the force error curves of Element 6 and Element 10 diverge severely, and the maximum absolute errors are 8.136 kN and 12.140 kN respectively. The difference of loading histories exerts great influence on the prediction accuracy and adaptability of the traditional ANN method. In UKF case, the force error curves of three elements fluctuate greatly in the early stage and tend to zero lines in the later stage. The maximum absolute errors are 22.147 kN, 16.590 kN and 7.915 kN respectively.

Table 5 summarizes the maximum absolute errors and *RMSD* of the restoring force prediction of BRBs at each story. In ANN1 case, the maximum absolute errors of restoring force prediction at each story fluctuate within [0.683 kN, 2.980 kN]. In ANN2 case, the maximum absolute error increases from 3.321 kN of Element 2 to 11.540 kN of Element 12. In particular, the *RMSD* of Element 12 at 25 s in ANN2 case reaches 2.022, which implies that the difference of loading histories has great influence on the effectiveness of the traditional ANN method. In UKF case, the maximum absolute error decreases gradually from 22.147 kN of Element 2 to 4.970 kN of Element 12, which suggests that the UKF method has good convergence. However, the *RMSD* (at 25 s) of Element 2 in UKF case is about 20 times that of Element 2 in ANN1 case. And the *RMSD* (at 25 s) of Element 12 in UKF case is about 2.3 times that of Element 12 in ANN1 case. The results show that the proposed method can effectively solve the problem that the UKF method cannot overcome the model gap, and it is an effective supplement and improvement of the UKF method. In addition, the average one-step time of the proposed method is 0.13 s, which meets the requirement of slow SPDHS.

3.3.2 Preliminary hybrid simulation results

In the preliminary hybrid simulation, only 2500 samples of Experimental Substructure including displacements and restoring forces are generated. These samples contain enough hysteresis information about the Experimental Substructure. When the model gap is unknown, ANN can be trained by these valuable data, the purpose of which is to learn the hysteresis information of the real model in advance and guarantee the prediction accuracy and stability of mode updating.

These samples are randomly divided into two parts: 75% for training and 25% for testing. An initialized ANN model is established and trained by Neural Network Toolbox in MATLAB. The training algorithm is selected as Levenberg-Marquardt algorithm which is the most effective training algorithm for ANN. The training process of ANN is illustrated in Fig. 9. It can be seen that after 795 iterations, the loss function is reduced to 6.69×10^{-8}, and the prediction accuracy is relatively high. Fig. 10 shows the dimensionless force history and hysteresis curve predicted by ANN in the preliminary hybrid simulation. It is noted that the displacements and restoring forces have been normalized to [0, 1]. The restoring force predicted by the pre-trained ANN model in the preliminary hybrid simulation is marked with “ANN3”. And the true value of restoring force from the 2500 samples is marked with “Reference1”.

As shown in Fig. 10, the hysteresis curve and restoring force history predicted by the pre-trained ANN model are in good agreement with the real ones. The results show that the parameters in the ANN structure can be properly trained with single preliminary hybrid simulation. The pre-trained ANN model is set as the initial model of nonlinear component in Numerical Substructure I for the subsequent online model updating in SPDHS.

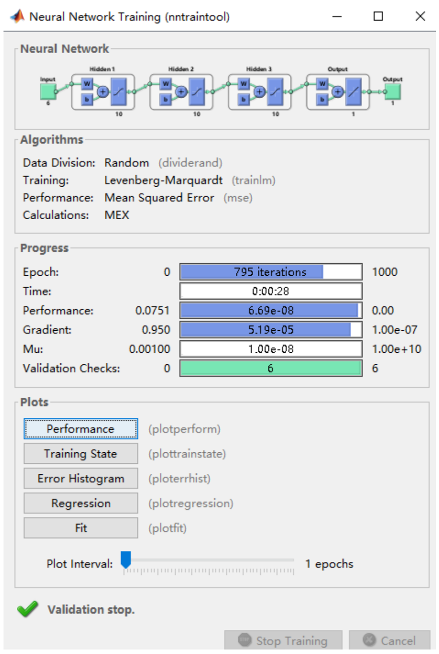

Fig. 9 Diagram of neural network training process

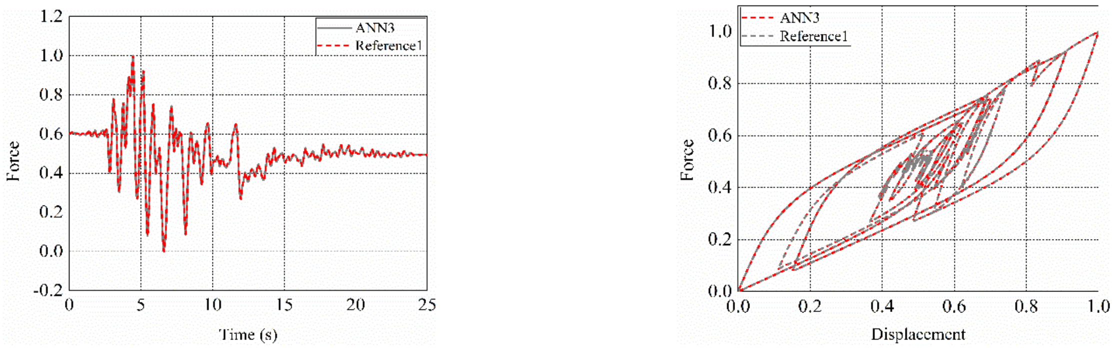

(a) Restoring force history (b) Hysteresis curve

Fig. 10 Restoring force history and hysteresis curve predicted by pre-trained ANN

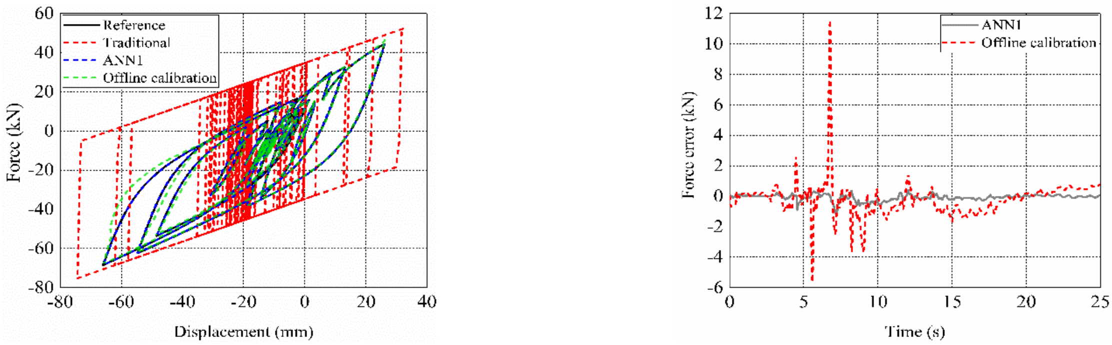

(a) Hysteresis curve (b) Restoring force prediction error curve

Fig. 11 Hysteresis curve and restoring force prediction error curve of Element 2

3.3.3 Performance of offline calibration

If preliminary hybrid simulation can be executed, and the models in Numerical Substructure I share similar characteristics with Experimental Substructure, it will be possible to offline calibrate the hysteresis models in Numerical Substructure I based on the pre-trained ANN model without online model updating. Thus, the offline calibration will be discussed in this section. Two simulation cases are compared as follows:

(a) Offline calibration case: The pre-trained ANN model in the preliminary hybrid simulation is set as the initial hysteresis model of element in Numerical Substructure I. Then the SPDHS is executed Offline calibration case: The pre-trained ANN model in the preliminary hybrid simulation is set as the initial hysteresis model of element in Numerical Substructure I . Then the SPDHS is executed without online model model updating. The results are marked with “Offline calibration”;

(b) ANN1 case: This simulation case is the same as the one in Section 3.3.1. And the results are marked with “ANN1”. The comparative simulation results are as follows:

Fig. 11 shows the hysteresis curve and restoring force prediction error curve of Element 2 in two simulation cases. It can be seen that, in some local regions, the hysteresis curve in offline calibration case deviates from the real model. The restoring force prediction error curve in ANN1 case tends to zero line. As a contrast, the restoring force prediction error in offline calibration case is larger than the one in ANN1 case in general. In particular, the maximum absolute error of restoring force prediction reaches to 11.230 kN at 6.52 s. Therefore, it is also needed to carry out subsequent online model updating to calibrate the pre-trained ANN model according to the Experimental substructure data.

3.3.4 The anti-noise ability of the proposed method

The effectiveness of the proposed method is verified by the above numerical simulation without experimental validation. The biggest difference between experiment and numerical simulation exists in noise, thus the anti-noise ability of the proposed method is evaluated in this section. Gauss white noise with different SNR (Signal to Noise Ratio) (5 db, 20 db, 40 db, 60 db) is added into the displacement and restoring force signals in ANN1 case. The predicted restoring force histories of three elements (Element 2, Element 6 and Element 10) with different SNR are illustrated in Fig. 12.

As seen in Fig. 12, after adding white noise of 5 dB, 20 dB, 40 dB and 60 dB to the response signals generated in ANN1 case, the predicted restoring force histories of three elements (Element 2, Element 6 and Element 10) coincide with the ones without noise. It is verified that the proposed method in this paper has good performance in resisting noise.

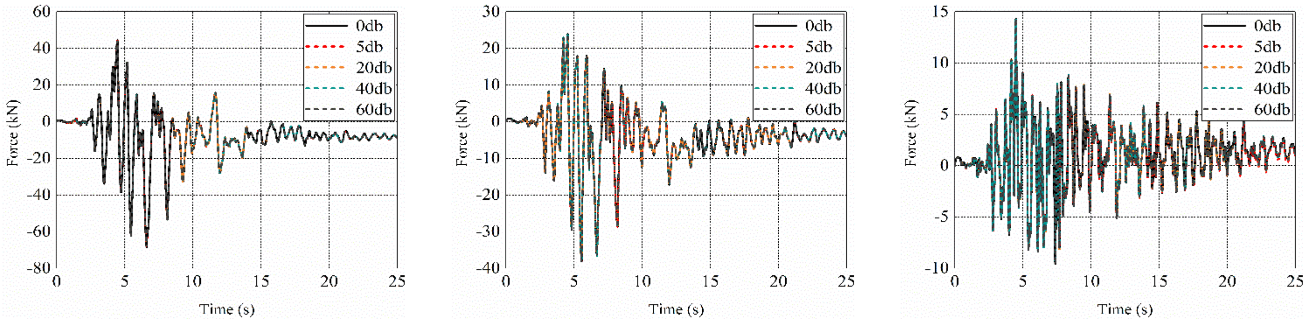

(a) Element 2 (b) Element 6 (c) Element 10

Fig. 12 Comparison of predicted restoring forces of three elements with different SNR in ANN1 case

3.3.5 Performance in another ground motion

To verify the effectiveness of the proposed method under different displacement histories, another different ground motion is selected to execute numerical simulation on the six-story structure with BRBs. The ground motion was recorded at in KAKOGAWA (CUE90) during the Kobe

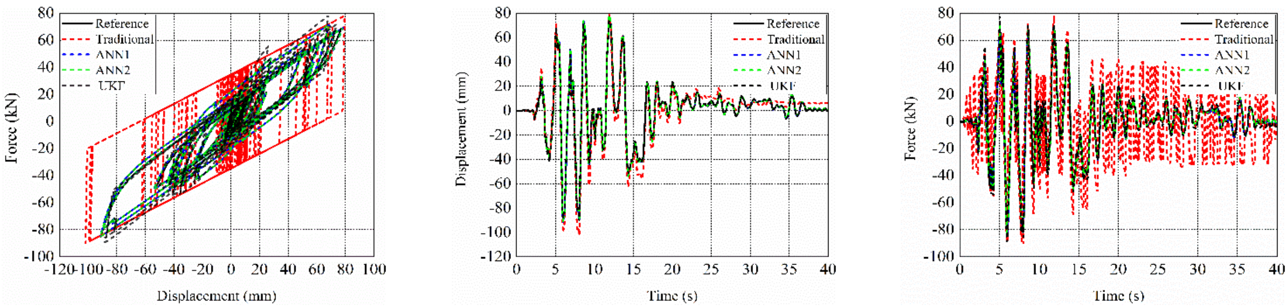

(a) Hysteresis curve (b) Displacement history (c) Restoring force history

Fig. 13 Comparison of predicted responses of Element 2 at the first story in different cases

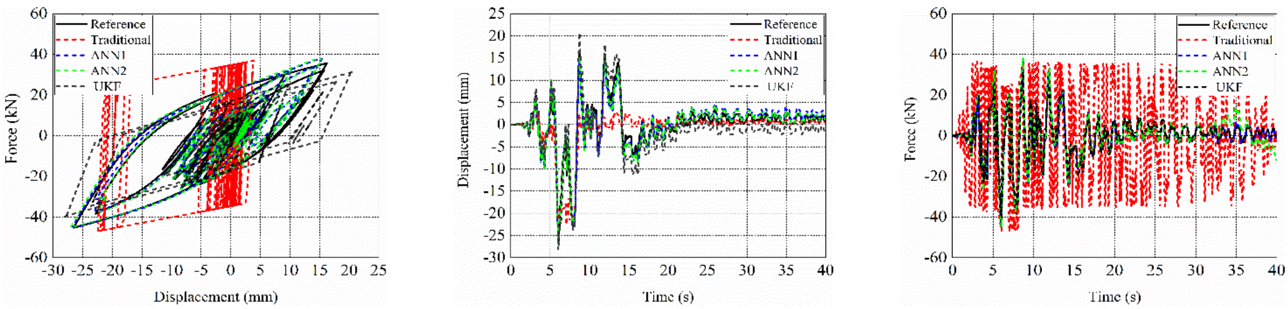

(a) Hysteresis curve (b) Displacement history (c) Restoring force history

Fig. 14 Comparison of predicted responses of Element 6 at the third story in different cases

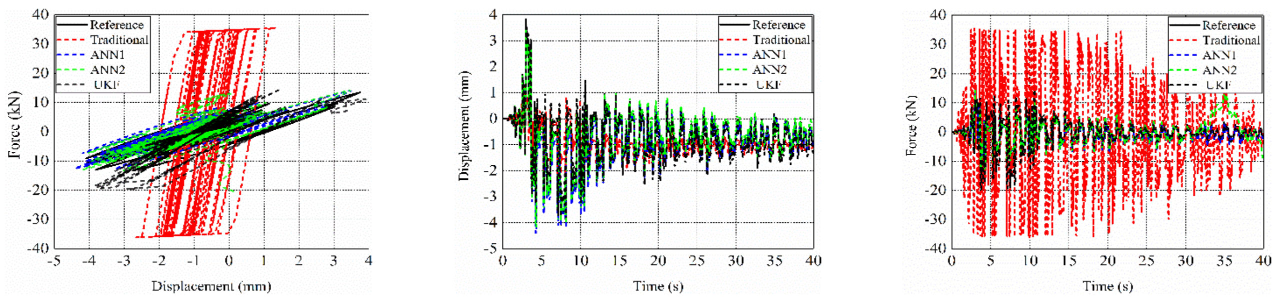

(a) Hysteresis curve (b) Displacement history (c) Restoring force history

Fig. 15 Comparison of predicted responses of Element 10 at the fifth story in different cases

(Japan) earthquake on January 16, 1995. Similarly, the peak acceleration is adjusted to 1000 gal and the sample time interval is set to 0.01 s. Comparison of the predicted hysteresis curves, displacement histories and restoring force histories of three elements (Element 2, Element 6 and Element 10) in five simulation cases are presented in Figs. 13-15. The simulation results are as follows:

As shown in Figs. 13-15, in ANN1 case, the hysteresis curves, displacement histories and restoring force histories are both in good agreement with the reference ones. It is demonstrated that the proposed method has good generality and model updating effects under another ground motion. In ANN2 case, due to the difference of loading histories, the restoring force histories of Element 6 and Element 10 deviate from the true value in the later stage. In UKF case, it is shown that the prediction errors cannot be ignored which are caused by the model gap between the initial numerical models and real ones.

4. Conclusions

The focus of this paper is to establish an online model updating method for SPDHS named artificial neural network (ANN) based on forgetting factor. Furthermore, the numerical analysis of a six-story structure with BRBs is conducted to verify the effectiveness and anti-noise ability of this method.

- Compared with the traditional ANN method, the proposed method in this paper has enough effectiveness in predicting the responses of elements when the loading histories with various characteristics are considered. It is verified that it has good adaptability and restoring force prediction accuracy.
- Compared with the UKF method, the proposed method reduces the model gap between the assumed numerical models and the real models, which demonstrates that the proposed method can improve the prediction accuracy of restoring force.
- The restoring force prediction of Elements 2-12 can still remain accurate when different white noise is added, which implies that the proposed method has good performance in resisting noise.

In conclusion, the proposed method can not only learn more hysteresis information which is not available in the initial numerical models, but also has good adaptability and accuracy in predicting the restoring force even under different loading histories.

Acknowledgments

The research described in this paper was financially supported by the Natural Science Foundation of China under grants No.51708110.

References

Baber, T.T. and Noori, M.N. (1985), "Random vibration of degrading, pinching systems", *J. Eng. Mech.*, **111**(8), 1010-1026. https://doi.org/10.1061/(ASCE)0733-9399(1985)111:8(1010)

Carrion, J.E., Spencer, B.F. and Phillips, B.M. (2009), "Real-time hybrid simulation for structural control performance assessment", *Earthq. Eng. Eng. Vib.*, **8**(4), 481-492. https://doi.org/10.1007/s11803-009-9122-4

Chen, C., Ricles, J.M., Marullo, T.M. and Mercan, O. (2009), "Real-time hybrid testing using the unconditionally stable explicit CR integration algorithm", *Earthq. Eng. Struct. Dyn.*, **38**(1), 23-44. https://doi.org/10.1002/eqe.838

Chuang, M.C., Hsieh, S.H., Tsai, K.C., Li, C.H., Wang, K.J. and Wu, A.C. (2018), "Parameter identification for on-line model updating in hybrid simulations using a gradient-based method", *Earthq. Eng. Struct. Dyn.*, **47**(2), 269-293. https://doi.org/10.1002/eqe.2950

Darby, A.P., Williams, M.S. and Blakeborough, A. (2002), "Stability and delay compensation for real-time substructure testing", *J. Eng. Mech.*, **128**(12), 1276-1284. https://doi.org/10.1061/(ASCE)0733-9399(2002)128:12(1276)

Dermitzakis, S.N. and Mahin, S.A. (1985), "Development of substructuring techniques for on-line computer controlled seismic performance testing", Ph.D. Dissertation; University of California, Berkeley, CA, USA.

Elanwar, H.H. and Elnashai, A.S. (2016), "Framework for online model updating in earthquake hybrid simulations", *J. Earthqu. Eng.*, **20**(1), 80-100. https://doi.org/10.1080/13632469.2015.1051637

Hashemi, M.J., Masroor, A. and Mosqueda, G. (2014), "Implementation of online model updating in hybrid simulation", *Earthq. Eng. Struct. Dyn.*, **43**(3), 395-412. https://doi.org/10.1002/eqe.2350

Kim, S.J., Holub, C.J. and Elnashai, A.S. (2011), "Experimental investigation of the behavior of RC bridge piers subjected to horizontal and vertical earthquake motion", *Eng. Struct.*, **33**(7), 2221-2235. https://doi.org/10.1016/j.engstruct.2011.03.013

Kim, J., Ghaboussi, J. and Elnashai, A.S. (2012), "hysteresis mechanical-informational modeling of bolted steel frame connections", *Eng. Struct.*, **45**, 1-11. https://doi.org/10.1016/j.engstruct.2012.06.014

Kwon, O. and Kammula, V. (2013), "Model updating method for substructure pseudo-dynamic hybrid simulation", *Earthq. Eng. Struct. Dyn.*, **42**(13), 1971-1984. https://doi.org/10.1002/eqe.2307

Kwon, O.S., Elnashai, A.S. and Spencer, B.F. (2008), "A famework for distributed analytical and hybrid simulations", *Struct. Eng. Mech., Int. J.*, **30**(3), 331-350. https://doi.org/10.12989/sem.2008.30.3.331

MATLAB Inc. (2018), http://www. mathworks. com

Moré, J.J. (1978), The Levenberg-Marquardt Algorithm: Implementation and Theory, In: *Numerical Analysis* (pp. 105-116), Springer, Berlin, Heidelberg, Germany. https://doi.org/10.1007/BFb0067700

Nakashima, M. and Takai, H. (1985), "Use of Substructure Techniques in Pseudo Dynamic Testing", Research Report No. R111; Building Research Institute, Ministry of Construction, Japan.

Nakashima, M., Kato, H. and Takaoka, E. (1992), "Development of real-time pseudo dynamic testing", *Earthq. Eng. Struct. Dyn.*, **21**(1), 79-92. https://doi.org/10.1002/eqe.4290210106

Ning, X.Z., Wu, B., Tan, Q.Y., Yang, G. and Xu, G.S. (2019), "Application of online numerical simulation method in BRB-RC frame structure", *J. Build. Struct.*, **40**(10), 86-92. [In Chinese] https://doi.org/10.14006/j. jzjgxb.2019.0071

Ou, G., Dyke, S.J. and Prakash, A. (2017), "Real time hybrid simulation with online model updating: An analysis of accuracy", *Mech. Syst. Signal Proc.*, **84**, 223-240. https://doi.org/10.1016/j.ymssp.2016.06.015

Phillips, B.M. and Spencer Jr, B.F. (2013), "Model-based feedforward-feedback actuator control for real-time hybrid simulation", *J. Struct. Eng.*, **139**(7), 1205-1214. https://doi.org/10.1061/(ASCE)ST.1943-541X.0000606

Schellenberg, A., Kim, H.K. and Takahashi, Y. (2009), *OpenFRESCO Command Language Manual*, University of California, Berkeley, CA, USA.

Shao, X., Mueller, A. and Mohammed, B.A. (2016), "Real-Time Hybrid Simulation with Online Model Updating: Methodology and Implementation", *J. Eng. Mech.*, **142**(2), 04015074. https://doi.org/10.1061/(ASCE)EM.1943-7889.0000987

Spencer, B.F., Chang, C.M., Frankie, T.M., Kuchma, D.A., Silva, P.F. and Abdelnaby, A.E. (2014), "A phased approach to enable hybrid simulation of complex structures", *Earthq. Eng. Eng. Vib.*, **13**(1), 63-77. https://doi.org/10.1007/s11803-014-0240-2

Tang, Z.Y., Chen, S.C., Zhang, J.X. and Li, Z.B. (2016), "Study on the stability prediction of real-time dynamic substructuring system based on shaking table", *Eng. Mech.*, **33**(12), 217-224. [In Chinese] https://doi.org/10.6052/j.issn.1000-4750.2015.08.0716

Wang, T. and Wu, B. (2013), "Hybrid testing method based on model updating with constrained unscented Kalman Filter", *J. Earthq. Eng. Eng. Vib.*, **33**(5), 100-109. [In Chinese] https://doi.org/10.13197/j.eeev.2013.05.100.wangt.013

Wang, T., Zhai, X.H., Meng, L.Y. and Wang, Z. (2017), "Hybrid testing method based on an online neural network algorithm", *J. Vib. Shock*, **36**(14), 1-8. [In Chinese] https://doi.org/10.13465/j.cnki.jvs.2017.14.001

Wang, Z., Ning, X., Xu, G., Zhou, H. and Wu, B. (2019), "High performance compensation using an adaptive strategy for real-time hybrid simulation", *Mech. Syst. Signal Proc.*, **133**, 106262. https://doi.org/10.1016/j.ymssp.2019.106262

Wu, B. and Wang, T. (2014), "Model updating with constrained unscented kalman filter for hybrid testing", *Smart. Struct. Syst., Int. J.*, **14**(6), 1105-1129. https://doi.org/10.12989/sss.2014.14.6.1105

Wu, B. and Zhou, H. (2014), "Sliding mode for equivalent force control in real-time substructure test", *Struct. Control. Health Monit.*, **21**(10), 1284-1303. https://doi.org/10.1002/stc.1648

Wu, B., Bao, H., Ou, J. and Tian, S. (2005), "Stability and accuracy analysis of the central difference method for real-time substructure testing", *Earthq. Eng. Struct. Dyn.*, **34**(7), 705-718. https://doi.org/10.1002/eqe.451

Wu, B., Xu, G., Wang, Q. and Williams, M.S. (2006), "Operator-splitting method for real-time substructure testing", *Earthq. Eng. Struct. Dyn.*, **35**(3), 293-314. https://doi.org/10.1002/eqe.519

Wu, B., Ning, X., Xu, G., Wang, Z., Mei, Z. and Yang, G. (2018), "Online numerical simulation: A hybrid simulation method for incomplete boundary conditions", *Earthq. Eng. Struct. Dyn.*, **47**(4), 889-905. https://doi.org/10.1002/eqe.2996

Yang, W.J. and Nakano, Y. (2005), "Substructure online test by using real-time hysteresis modeling with a neural network", *Adv. Experim. Struct. Eng.*, **38**, 267-274.

Yang, Y.S., Tsai, K.C., Elnashai, A.S. and Hsieh, T.J. (2012), "An online optimization method for bridge dynamic hybrid simulations", *Simul. Model. Pract. Theory*, **28**, 42-54. https://doi.org/10.1016/j.simpat.2012.06.002

Yun, G.J., Ghaboussi, J. and Elnashai, A.S. (2008a), "A new neural network-based model for hysteresis behavior of materials", *Int. J. Numer. Meth. Eng.*, **73**(4), 447-469. https://doi.org/10.1002/nme.2082

Yun, G.J., Ghaboussi, J. and Elnashai, A.S. (2008b), "Self-learning simulation method for inverse nonlinear modeling of cyclic behavior of connections", *Comput. Meth. Appl. Mech. Eng.*, **197**(33-40), 2836-2857. https://doi.org/10.1016/j.cma.2008.01.021

Zakersalehi, M., Tasnimi, A.A. and Ahmadizadeh, M. (2019), "Reliable nonlinear hybrid simulation using modified operator splitting technique", *Struct. Control. Health Monit.*, **26**(1), e2283. https://doi.org/10.1002/stc.2283

Zhang, J., Wu, B. and Wang, T. (2011), "Adaptive substructure testing method based on least square", *Proceedings of International Conference on Electric Technology and Civil Engineering* (*ICETCE*), IEEE. https://doi.org/10.1109/ICETCE.2011.5775338

BS